Int J Theor Phys (2010) 49: 2540–2557
DOI 10.1007/s10773-010-0446-7

Space-Time Dynamics of Gazeau-Klauder Coherent States in Power-Law Potentials

Shahid Iqbal · Paula Rivière · Farhan Saif

Received: 22 April 2010 / Accepted: 22 July 2010 / Published online: 19 August 2010

Abstract Gazeau-Klauder coherent states are developed for power-law potentials and their evolution in space and time is analyzed. We show that these states follow classical dynamics as long as the underlying energy spectrum is linear, otherwise they follow a classical-like evolution upto a few classical periods and disperse thereafter, despite its special construction. Auto-correlation function and probability density as a function of space and time explain the spatio-temporal behavior of these states.

Keywords Gazeau-Klauder coherent states · Generalized coherent states · Space-time dynamics · Temporal stability · Quantum revivals · Quantum carpets · Power-law potentials · Loosely binding potentials · Tightly binding potentials · Auto-correlation function · Probability density function

1 Introduction

In 1926 Erwin Schrödinger attempted to build quantum mechanical states which follow classical trajectories and obey minimum uncertainty relationship, i.e., nondispersive wave packets [1]. He succeeded for the harmonic oscillator, obtaining for the first time a one-to-one correspondence between wave packet and classical particle. In 1963, the ground breaking work of Roy Glauber, in the context of quantum theory of light, introduced electromagnetic field states which resemble the classical field [2–4], and named them coherent states (CS). Glauber introduced three definitions of coherent states: (i) the coherent states $|z\rangle$ are the

S. Iqbal (✉) · F. Saif
Department of Electronics, Quaid-i-Azam University, Islamabad 45320, Pakistan
e-mail: sic80@hotmail.com

F. Saif
e-mail: farhan.saif@fulbrightmail.org

S. Iqbal · P. Rivière
Max-Planck Institute for the Physics of Complex Systems, Nöthnitzer Straße 38, 01187 Dresden, Germany

eigen states of the harmonic oscillator annihilation operator; (ii) they are states generated by the action of unitary z-displacement ($z \in \mathcal{C}$) on the vacuum state of the harmonic oscillator; and (iii) they are the quantum states which minimize the uncertainty relation. These states are associated with the Heisenberg-Weyl algebra in terms of the harmonic oscillator annihilation and creation operators. These three definitions are equivalent and the so obtained coherent state possesses a special set of properties, such as (a) continuity in parameters; (b) resolution of unity; and (c) minimizing the uncertainty relationship, which remains minimum under time evolution [2–4]. Nondispersive quantum states for more general physical systems, however, remained a dream of Erwin Shrödinger.

Because of their abundant applications [5–8], there have been continuous efforts to extend the notion of coherent states to other general physical systems. The early generalizations were based on group theoretic approaches and CSs have been constructed for a variety of algebraic groups, such as Lie groups $SU(1,1)$ [9] and non-compact groups $SO(2,1)$ [10, 11] following definitions (i) and (ii), respectively. The CSs based on such generalizations are continuously parameterized and admit the resolution of unity, which are two main characteristics of Glauber's CS.

In 1996 Klauder suggested a new type of coherent states suitable for systems with degenerate discrete spectra (i.e. the hydrogen atom) without an explicit dependence on any group structure [12]. In Klauder's opinion, these states possess the properties of Glauber's CS, as expressed above, hence, the long-standing problem of finding nondispersive wave packets for hydrogen atom, was considered as solved. In [13] it is shown that these Klauder states are dispersive in nature for the hydrogen atom.

Gazeau and Klauder extended the idea of *temporally stable* CSs for non-degenerate discrete and continuous spectra [14]. This formalism attracted much more attention due to its independence on the groups, and these coherent states have been built for a variety of Hamiltonian systems, such as, the pseudoharmonic oscillator [15], the Morse potential [16, 17], the Pöschl-Teller potential and the infinite square well [18], and one-mode systems with periodic potentials [19]. The present work is focussed on Gazeau and Klauder coherent states (GK CSs) in a general class of one-dimensional potentials known as power-law potentials and on their dynamical characteristics. Power-law potentials (PLPs) are categorized as loosely binding potentials and tightly binding potentials, and the harmonic potential serves as a boundary between them [20]. We analyze the temporal evolution of GK CSs on the basis of the underlying energy spectrum of the physical system by means of the autocorrelation function and the probability density function. We show that: (i) these states evolve in time without dispersion as long as the underlying energy spectrum is linear; (ii) they otherwise disperse and exhibit quantum features such as quantum revivals and fractional revivals; (iii) non-trivial space-time dynamics results the formation of quantum carpets [21, 22]; and (iv) the special construction of quantum states following GK CSs formalism does not overcome the inherent dispersion of dynamical system with nonlinear energy spectrum.

The paper is organized as follows: In Sect. 2, we briefly describe PLPs and their underlying energy spectra. In Sect. 3, we construct GK CSs for power-law potentials and discuss their basic characteristics. In Sect. 4, we analyze the temporal evolution of GK CSs. We discuss the harmonic oscillator, the infinite square well and triangular well potential as examples of the power-law potentials.

2 General Power-Law Potentials (PLPs)

A general class of potentials, defined by the power-law exponent, may effectively be divided into two types: loosely binding potentials, for which the energy level spacing re-

duces with increasing quantum number; and, tightly binding potentials, for which the energy level spacing increases with increasing quantum number [20]. The general form of the one-dimensional power-law potentials is [23]

$$V^{(k)}(x) = V_0 \left| \frac{x}{a} \right|^k, \tag{1}$$

where, V_0 and a are constants, respectively, with dimensions of energy and length. The power-law exponent k determines the type of potential, hence, for $k > 2$, we find tightly binding potentials, and $k < 2$ corresponds to loosely binding potentials, whereas, the harmonic oscillator potential appears for $k = 2$ and thus separates the two kind of potentials. The corresponding general Hamiltonian, becomes

$$\hat{H}^{(k)} = \frac{\hat{p}^2}{2m} + \hat{V}^{(k)}(x), \tag{2}$$

which obeys the eigenvalue equation

$$\hat{H}^{(k)}|n\rangle = E_n^{(k)}|n\rangle, \quad n \geq 0. \tag{3}$$

The eigenenergies, $E_n^{(k)}$, can be obtained within the WKB approximation [20, 23], such that,

$$E_n^{(k)} = \omega^{(k)} \left(n + \frac{\gamma}{4} \right)^{2k/(k+2)}, \tag{4}$$

where

$$\omega^{(k)} = \left[\frac{\hbar\pi}{2a\sqrt{2m}} V_0^{1/k} \frac{\Gamma(1/k + 3/2)}{\Gamma(1/k + 1)\Gamma(3/2)} \right]^{2k/(k+2)}, \tag{5}$$

has dimensions of energy for any particular value of k. The eigenenergies in (4) do indeed give the large n behavior of symmetric one-dimensional PLPs. Here, γ is the Maslov index, which accounts for boundary effects at the classical turning points [20]. In order to gain insight into the structure of the energy spectrum given by (4), we take the energy difference between any two adjacent levels,

$$\Delta E_n^{(k)} = E_n^{(k)} - E_{n-1}^{(k)} = \omega^{(k)} \left(\frac{2k}{k+2} \right) \left(n + \frac{\gamma}{4} \right)^{\frac{k-2}{k+2}}. \tag{6}$$

Equation (6) shows that for $k = 2$, $\Delta E_n^{(k)}$ does not depend on n, so the energy spectrum is equally spaced. For $k > 2$, the energy difference between adjacent levels increases with n (tightly binding potentials), while for $k < 2$, it decreases with n (loosely binding potentials).

The general Hamiltonian $\hat{H}^{(k)}$ is rewritten as

$$\hat{H}^{(k)} = \omega^{(k)} \hat{X}_N^{(k)}, \tag{7}$$

where, $\omega^{(k)}$ is defined in (5) and $\hat{X}_N^{(k)}$ follows the eigenvalue equation

$$\hat{X}_N^{(k)}|n\rangle = e_n^{(k)}|n\rangle. \tag{8}$$

The dimensionless eigenvalues are obtained as

$$e_n^{(k)} = \frac{E_n^{(k)} - E_0^{(k)}}{\omega^{(k)}} = \left(n + \frac{\gamma}{4}\right)^{2k/(k+2)} - \left(\frac{\gamma}{4}\right)^{2k/(k+2)}, \tag{9}$$

which are increasing function of n, such that, $e_{n+1}^{(k)} > e_n^{(k)}$, with $e_0^{(k)} = 0$.

Equation (1) defines the harmonic oscillator potential for $k = 2$ (with $V_0/a^2 = m\Omega^2/2$) and the infinite square well potential for $k \to \infty$ (any V_0), which is an example of tightly binding potentials. The corresponding eigenenergies are, respectively

$$E_n^{(2)} = \hbar\Omega\left(n + \frac{1}{2}\right),$$

and

$$E_n^{(\infty)} = \frac{\hbar^2\pi^2}{8a^2m}(n+1)^2,$$

Here, the Maslov index γ takes the values, such that, $\gamma = 2$ for the harmonic oscillator, and $\gamma = 4$ for the infinite square well [20].

A quantum bouncer or triangular well potential [24, 25], being the example of loosely binding potentials, is defined for $k = 1$, that is

$$\begin{aligned} V(x) &= mgx, \quad x > 0 \\ &= \infty, \quad x \le 0. \end{aligned} \tag{10}$$

The solutions to the corresponding time independent Schrödinger wave equation [24, 25], are displaced Airy functions, that is, $\psi_n(\zeta) = N_n\,\mathrm{Ai}(\zeta - \zeta_n)$, where N_n is the normalization factor, and $\zeta = x/x_0$, where $x_0 = (\hbar^2/2gm^2)^{1/3}$. Moreover, $\zeta_n = E_n/(mgx_0)$, is the n-th negative zero of the Airy function, with $n = 1, 2, 3, \ldots$, and, $\zeta_n > 0$. Applying the boundary condition, that is, $\psi_n(0) = \mathrm{Ai}(-\zeta_n) = 0$ at $\zeta = 0$, we find zeros ζ_n, and the normalization factor, N_n [24, 25], as

$$\zeta_n = \left[\frac{3\pi}{2}\left(n - \frac{1}{4}\right)\right]^{2/3}, \tag{11}$$

and

$$N_n = \left[\frac{2}{3}\frac{\pi^2}{(n-1/4)}\right]^{1/6}. \tag{12}$$

We find the eigenenergy in terms of physical parameters as

$$E_n = \omega_0\left(n - \frac{1}{4}\right)^{2/3}, \tag{13}$$

where, $\omega_0 = (3\sqrt{m}\hbar g\pi/2\sqrt{2})^{2/3}$. It is interesting to note that at large n, (4) is completely equivalent to (13) for $k = 1$ and $V_0/a = mg$ as we replace $2a$ by a due to truncation of the symmetric power-law potential at $x = 0$.

3 GK Coherent States for PLPs

The Gazeau and Klauder formalism [14] to construct coherent states of Hamiltonians with discrete and non-degenerate energy spectra without any explicit dependence on group properties is based on two real parameters, J and θ, with $J \geq 0$ and $-\infty < \theta < \infty$. For general power-law potentials, GK CSs have the form,

$$\left|(J,\theta)^{(k)}\right\rangle = \frac{1}{\sqrt{N^{(k)}(J)}} \sum_{n=0}^{\infty} \frac{J^{\frac{n}{2}} e^{-ie_n^{(k)}\theta}}{\sqrt{\rho_n^{(k)}}} |n\rangle. \tag{14}$$

The coherent states are based on eigenenergies obtained via WKB method given in (4). The quantity $\rho_n^{(k)}$ is defined in terms of $e_n^{(k)}$, given by (9), so that

$$\rho_n^{(k)} \equiv \prod_{j=1}^{n} e_j^{(k)} = \prod_{j=1}^{n} \left[\left(j + \frac{\gamma}{4} \right)^{2k/(k+2)} - \left(\frac{\gamma}{4} \right)^{2k/(k+2)} \right]. \tag{15}$$

Following Gazeau and Klauder's definitions, CSs display the characteristics [12, 14] of (a) normalization; (b) continuity in J and θ; (c) resolution of unity; (d) action identity, and (e) temporal stability. In our latter discussion we explain these characteristics for the GK CSs given in (14): The normalization condition $\langle (J,\theta)^{(k)} \big| (J,\theta)^{(k)} \rangle = 1$ provides the normalization constant as

$$N^{(k)}(J) = \sum_{n=0}^{\infty} \frac{J^n}{\rho_n^{(k)}}. \tag{16}$$

Furthermore, the overlap of two GK CSs can be written as

$$\left\langle (J',\theta')^{(k)} | (J,\theta)^{(k)} \right\rangle = \frac{1}{\sqrt{N^{(k)}(J')}\sqrt{N^{(k)}(J)}} \sum_{n=0}^{\infty} \frac{(J'J)^n}{\rho_n^{(k)}} e^{-i(\theta-\theta')e_n^{(k)}}.$$

The continuity in two labels J and θ follows from the continuity of the overlap $\langle (J',\theta')^{(k)} | (J,\theta)^{(k)} \rangle$, because

$$\left\| \left|(J,\theta)^{(k)}\right\rangle - \left|(J',\theta')^{(k)}\right\rangle \right\|^2 = 2\left[1 - \mathrm{Re}\left\langle (J',\theta')^{(k)} \middle| (J,\theta)^{(k)} \right\rangle\right] \tag{17}$$

approaches zero as $(J',\theta') \to (J,\theta)$.

However, for the resolution of unity, we take an integration measure $d\mu(J,\theta)$ [14], such that,

$$\int d\mu(J,\theta) \left|(J,\theta)^{(k)}\right\rangle \left\langle (J,\theta)^{(k)}\right| = \lim_{\Gamma\to\infty} \frac{1}{2\Gamma} \int_0^R dJ h(J) \int_{-\Gamma}^{\Gamma} d\theta \left|(J,\theta)^{(k)}\right\rangle \left\langle (J,\theta)^{(k)}\right|, \tag{18}$$

where $h(J)$ is defined [14] as

$$h(J) = N^{(k)}(J) w^{(k)}(J), \quad 0 \leq J < R,$$

which is specified by a proper choice of the probability distribution function, $w^k(J)$. The range of allowed values of J, i.e., $0 \leq J < R$, is determined by the radius of convergence,

$$R = \lim_{n\to\infty} \sqrt[n]{\rho_n^{(k)}} = \infty,$$

for $k > 0$. In order to calculate the resolution of unity, integration over θ, in (18), provides

$$\lim_{\Gamma\to\infty}\frac{1}{2\Gamma}\int_{-\Gamma}^{\Gamma}(.)d\theta = \delta_{e_n^{(k)},e_m^{(k)}},$$

which can be identified with the Kronecker delta $\delta_{n,m}$, due to the non-degeneracy of the energy spectrum [14]. Therefore, we write (18) as

$$\int d\mu(J,\theta)\big|(J,\theta)^{(k)}\big\rangle\big\langle(J,\theta)^{(k)}\big| = I$$
$$= \sum_{n=0}^{\infty}\frac{1}{\rho_n^{(k)}}\left\{\int_0^{\infty}\frac{h(J)}{N^{(k)}(J)}J^n dJ\right\}|n\rangle\langle n|,$$

provided there is a function $w^{(k)}(J)$ which satisfies

$$\int_0^{\infty} J^n w^{(k)}(J)dJ = \rho_n^{(k)}. \tag{19}$$

The positive constants $\rho_n^{(k)}$ are then power moments of the function $w^{(k)}(J)$. For an appropriate choice of $w^{(k)}(J)$ [26], the integral in (19) becomes a Stieltjes moment problem that can be solved using Mellin and inverse Mellin transformations.

The action identity is obtained from (9) and (15),

$$\big\langle(J,\theta)^{(k)}\big|\hat{H}\big|(J,\theta)^{(k)}\big\rangle = \frac{\omega^{(k)}}{N^{(k)}(J)}\sum_{n=0}^{\infty}\frac{J^n}{\rho_n^{(k)}}e_n^{(k)} = \omega^{(k)}J,$$

where we have used [14] $\rho_0^{(k)} = 1$.

4 Spatio-Temporal evolution of GK CSs in PLPs

The coherent states of the harmonic oscillator [1–4] are purely quantum mechanical in construction, but close to classical in behavior as they follow classical trajectories in their time evolution. The question whether this behavior can be generalized to coherent states for general potentials has historically aroused a great interest. In order to answer the question we study the time evolution of GK CSs for PLPs and explain our analytically and numerically obtained results. We write the time evolution operator for these states as

$$\hat{U}(t) = \exp[-i\omega^{(k)}\hat{X}_N^{(k)}t]. \tag{20}$$

The time evolution operator transforms the states from an initial time i.e., $t_0 = 0$ to any latter time, t, such that

$$\hat{U}^{(k)}(t)\big|(J,\theta)^{(k)}\big\rangle = \big|(J,\theta)^{(k)},t\big\rangle.$$

We may express the time evolved states $|(J,\theta)^{(k)},t\rangle$ as

$$\big|(J,\theta)^{(k)},t\big\rangle = \frac{1}{\sqrt{N^{(k)}(J)}}\sum_{n=0}^{\infty}\frac{J^{\frac{n}{2}}e^{-ie_n^{(k)}(\theta+\omega^{(k)}t)}}{\sqrt{\rho_n^{(k)}}}|n\rangle. \tag{21}$$

For the special case, in which $e_n^{(k)}$ has linear dependence on the quantum number, n, i.e., $e_n^{(k)} \propto n$, the time evolution of the coherent states $|(J,\theta)^{(k)}\rangle$ reduces to a rotation in complex plane,

$$\hat{U}^{(k)}(t)\big|(J,\theta)^{(k)}\big\rangle = \big|(J,\theta)^{(k)} e^{-i\omega^{(k)}t}\big\rangle,$$

thus the time evolved coherent state, $|(J,\theta)^{(k)},t\rangle$, is the same coherent state with a difference of a constant phase [1–4]. However, in general, the nonlinear dependence of the eigenenergy $e_n^{(k)}$ on quantum number, n, causes a transition to non-classical phenomena, such as, quantum revivals and fractional revivals, during the time evolution of GK CSs. The time evolution of these states, as defined by the time evolution operator in (20), is explained using the auto-correlation function [27], that is,

$$A(t) = \big\langle (J,\theta)^{(k)}\big|e^{-i\omega^{(k)}\hat{X}_N^{(k)}t}\big|(J,\theta)^{(k)}\big\rangle. \tag{22}$$

In order to calculate the auto-correlation function we use (8) and (14) to get

$$A(t) = \sum_{n=0}^{\infty}\big|c_n^{(k)}\big|^2 e^{-i\varepsilon_n^{(k)}t},$$

where, $\varepsilon_n^{(k)} \equiv \omega^{(k)} e_n^{(k)}$, and the weighting distribution $|c_n^{(k)}|^2$ is

$$\big|c_n^{(k)}\big|^2 \equiv \big|\langle n|(J,\theta)^{(k)}\rangle\big|^2 = \frac{1}{N^{(k)}(J)}\frac{J^n}{\rho_n^{(k)}}, \tag{23}$$

which determines the initial localization of the GK CSs with mean value

$$\langle n\rangle \equiv \big\langle (J,\theta)^{(k)}\big|\hat{N}\big|(J,\theta)^{(k)}\big\rangle = \frac{1}{N^{(k)}(J)}\sum_{n=0}^{\infty}\frac{nJ^n}{\rho_n^{(k)}}, \tag{24}$$

and spread $\Delta n = (\langle n^2\rangle - \langle n\rangle^2)^{1/2}$, where $\langle n^2\rangle = \langle (J,\theta)^{(k)}|\hat{N}^2|(J,\theta)^{(k)}\rangle$, and, $\hat{N}$ is the number operator. It is important to note that, for a particular value of the exponent k, the weighting distribution $|c_n^{(k)}|^2$ depends only on the parameter J, such that its mean value, $\langle n\rangle$, increases with J as seen in Fig. 1 and vice versa. For our latter numerical calculations, we choose four values of parameter J, such that the corresponding weighting distributions take the mean value $\langle n\rangle \simeq 5, 10, 15, 30$.

For GK CSs, initially narrowly peaked around the mean value $\langle n\rangle$, and with a spread $\Delta n \ll \langle n\rangle$, we use Taylor expansion for $\varepsilon_n^{(k)}$ around the mean quantum number, such that

$$\varepsilon_n^{(k)} - \varepsilon_{\langle n\rangle}^{(k)} = \sum_{r=1}^{\infty}\frac{1}{r!}\frac{\partial^r \varepsilon_n^{(k)}}{\partial n^r}\bigg|_{n=\langle n\rangle}(n-\langle n\rangle)^r, \tag{25}$$

where each term defines a time scale [28, 29], that is,

$$T_{(r)}^{(k)} = 2\pi\left(\frac{1}{r!}\left|\frac{\partial^r \varepsilon_n^{(k)}}{\partial n^r}\right|_{n=\langle n\rangle}\right)^{-1}. \tag{26}$$

For $r = 1, 2, 3$ these time scales define classical period, quantum revival and super revival times, respectively, written as $T_{(1)}^{(k)} = T_{cl}^{(k)}$, $T_{(2)}^{(k)} = T_{rev}^{(k)}$, and $T_{(3)}^{(k)} = T_{sr}^{(k)}$, such that, $T_{cl}^{(k)} <$

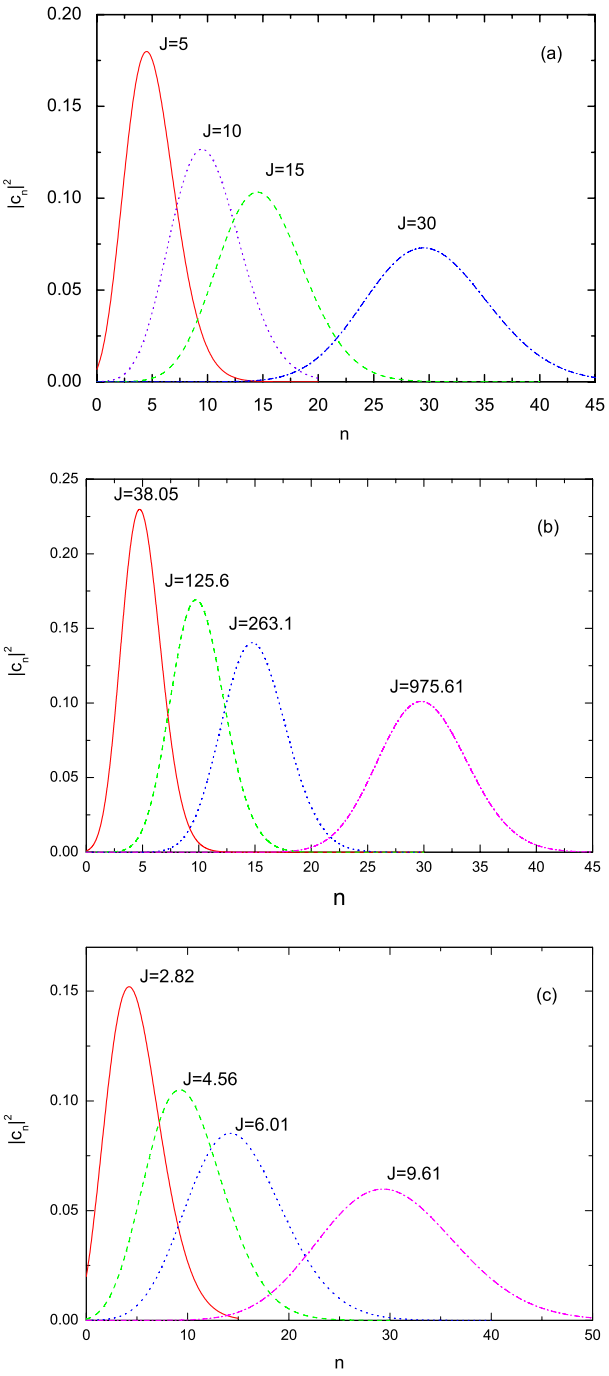

Fig. 1 The weighting distributions $|c_n^{(k)}|^2$ as given in (23) are plotted as a function of n for different values of J. The values of J are so chosen that distributions take the mean $\langle n\rangle \simeq 5, 10, 15, 30$, respectively, for (**a**) Harmonic oscillator ($k = 2$) $J = 5, 10, 15, 30$, (**b**) infinite square well ($k \to \infty$) $J = 38.05, 125.6, 263.1, 975.61$, and (**c**) triangular well potential ($k = 1$), $J = 2.82, 4.56, 6.01, 9.61$. In our numerical calculations we have considered the maximum value of quantum number n as $n_{max} = 100$

$T_{rev}^{(k)} < T_{sr}^{(k)}$ [28, 29]. Hence, (5) and (9) lead us to calculate the classical period $T_{cl}^{(k)}$, the quantum revival time $T_{rev}^{(k)}$, and the super revival time $T_{sr}^{(k)}$ as

$$T_{cl}^{(k)} = \frac{\pi}{\omega^{(k)}} \left| \frac{(k+2)}{k} \right| \left(\langle n \rangle + \frac{\gamma}{4} \right)^{-(k-2)/(k+2)}, \tag{27}$$

$$T_{rev}^{(k)} = \frac{2\pi}{\omega^{(k)}} \left| \frac{(k+2)^2}{k(k-2)} \right| \left(\langle n \rangle + \frac{\gamma}{4} \right)^{4/(k+2)}, \tag{28}$$

$$T_{sr}^{(k)} = \frac{3\pi}{2\omega^{(k)}} \left| \frac{(k+2)^3}{k(k-2)} \right| \left(\langle n \rangle + \frac{\gamma}{4} \right)^{(k+6)/(k+2)}. \tag{29}$$

The quantum revival time $T_{rev}^{(k)}$ and super revival time $T_{sr}^{(k)}$ approach infinity for $k = 2$. Therefore, the GK CSs for $k = 2$, which are precisely the coherent states of the harmonic oscillator, follow classical trajectories only with a periodicity defined by classical time period, $T_{cl}^{(2)}$: there is no dispersion. This nondispersive evolution, as depicted in Fig. 2, is due to the fact that the energy levels are equally spaced. However, as exponent deviates from $k = 2$, nonlinearity enters in the energy spectrum. In this situation, $T_{rev}^{(k)}$ takes a finite value, and the GK CSs disperse during their time evolution. In general, we observe a collapse for GK CSs when there is a total dephasing between the evolution of the different contributions to the sum, and at $T_{rev}^{(k)}$ they tend to relocalize. The phenomena of collapse and revivals of GK CSs are shown in Figs. 3 and 6 for $k \neq 2$. Moreover, the classical period, $T_{cl}^{(k)}$, quantum revival time, $T_{rev}^{(k)}$, and super revival time $T_{sr}^{(k)}$, reflect the dependence on parameter, J, through the mean value, $\langle n \rangle$, as shown by (24) and (27–29).

In order to analyze the spatio-temporal evolution of GK CSs we study as well the probability density in space and time. The GK CSs display constructive and destructive interference following the relation,

$$2\,\mathrm{Re}\left[\frac{1}{N^{(k)}(J)} \sum_{m \neq n}^{\infty} \frac{J^{\frac{(n+m)}{2}}}{\sqrt{\rho_n^{(k)} \rho_m^{(k)}}} \psi_n^{(k)}(x) \psi_m^{*(k)}(x) e^{-i(e_n^{(k)} - e_m^{(k)})(\theta + \omega^{(k)} t)} \right],$$

where $\psi_n^{(k)}(x)$ are the eigenstates for power-law potentials defined in position space. The space-time evolution of the probability density, hence, depend both on the nature of the eigenstates $\psi_n^{(k)}(x)$ and on the structure of the energy spectrum $e_n^{(k)}$ of the physical system, and therefore defines the interference behavior. A constant background independent of time is obtained from

$$\frac{1}{N^{(k)}(J)} \sum_{n=m}^{\infty} \frac{J^n}{\rho_n^{(k)}} \left| \psi_n^{(k)}(x) \right|^2.$$

In the following we consider some particular cases of power-law potentials and discuss their spatio-temporal evolution.

4.1 Harmonic Oscillator

For a power-law exponent $k = 2$, we find $e_n^{(2)} = n$ and $\rho_n^{(2)} = n!$, from (9) and (15), respectively. Thus the GK CS for the present obtained as,

$$\left| (J, \theta)^{(2)} \right\rangle = \frac{1}{\sqrt{N^{(2)}(J)}} \sum_{n=0}^{\infty} \frac{J^{\frac{n}{2}} e^{-in\theta}}{\sqrt{n!}} |n\rangle, \tag{30}$$

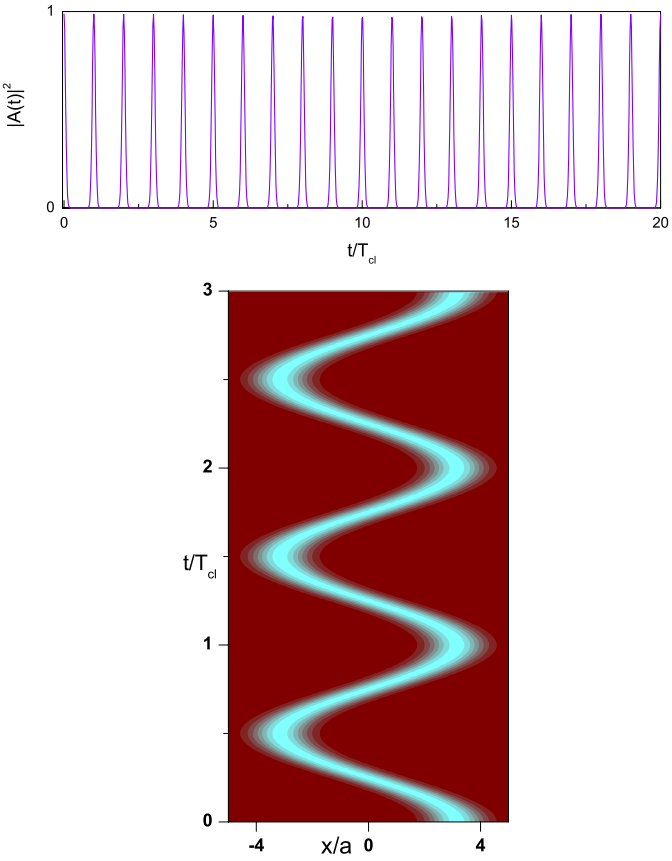

Fig. 2 We show the space-time evolution of GK CS of harmonic oscillator, given in (30), for $J = 5$: (**a**) modulus square of autocorrelation function, $|A(t)|^2$, given in (22), for $(k = 2)$ as a function of time, t. (**b**) Contour plot of probability density, $P^{(2)}(x,t) = |\langle x|e^{-i\omega^{(2)}\hat{X}_N^{(2)}t}|(J,\theta)^{(2)}\rangle|^2$, as a function of space and time (x,t)

where the normalization constant $N^{(2)}(J)$ is,

$$N^{(2)}(J) = \sum_{n=0}^{\infty} \frac{J^n}{n!}, \tag{31}$$

and the weighting distribution, given in (23), takes the form

$$|c_n^{(2)}|^2 = \frac{1}{N^{(2)}(J)} \frac{J^n}{n!}. \tag{32}$$

A transformation from (J,θ) to z, such that, $z = \sqrt{J}e^{-i\theta}$, introduces a complete equivalence between GK CS of the harmonic oscillator, given by (30), and Glauber's CS [2–4]. In this case, the normalization factor in (31) is $N^{(2)}(J) = e^{|z|^2}$, and the weighting distribution in (32) is $|c_n^{(2)}|^2 = |z|^{2n}e^{-|z|^2}/n!$ which is a Poisson distribution as for Glauber's CS. The time

evolution of GK CS for $k=2$, as written in (30), is obtained as

$$\left|(J,\theta)^{(2)},t\right\rangle = \frac{1}{\sqrt{N^{(2)}(J)}}\sum_{n=0}^{\infty}\frac{J^{\frac{n}{2}}e^{-in(\theta+\omega^{(2)}t)}}{\sqrt{n!}}|n\rangle$$
$$= \left|(J,\theta)^{(2)}e^{-i\omega^{(2)}t}\right\rangle. \tag{33}$$

In its time evolution, $|(J,\theta)^{(2)},t\rangle$ display a complete reconstruction at $T_{cl}^{(2)}=2\pi$ and no dispersion takes place, as shown in Fig. 2. It is supported by our analytical calculations which yield (from (27–29)) that $T_{cl}^{(2)}=2\pi$, whereas, $T_{rev}^{(2)}=T_{sr}^{(2)}=\infty$. It is worth noting that $T_{cl}^{(2)}$ is independent of the mean value, $\langle n\rangle$ and, thus, it does not depend on J. The particular behavior is a consequence of the inverse dependence of $T_{cl}^{(k)}$ on energy difference between adjacent n values, which is constant for $k=2$. Thus, $|(J,\theta)^{(2)},t\rangle$ has the same modulus of the amplitude as that of $|(J,\theta)^{(2)},0\rangle$ and differs only by a phase factor.

4.2 Infinite Square Well

The limiting case, $k\to\infty$, defines an infinite square well as seen from (1). Thus, eigenvalues $e_n^{(\infty)}=n(n+2)$, and the parameter $\rho_n^{(\infty)}=n!(n+2)!/2$ are obtained, respectively, from (9) and (15). The GK CS is, therefore, written as

$$\left|(J,\theta)^{(\infty)}\right\rangle = \frac{1}{\sqrt{N^{(\infty)}(J)}}\sum_{n=0}^{\infty}\frac{J^{\frac{n}{2}}e^{-in(n+2)\theta}}{\sqrt{n!(n+2)!/2}}|n\rangle, \tag{34}$$

with the normalization factor

$$N^{(\infty)}(J)=2\sum_{n=0}^{\infty}\frac{J^n}{n!(n+2)!},$$

and weighting distribution

$$\left|c_n^{(\infty)}\right|^2=\frac{2}{N^{(\infty)}(J)}\frac{J^n}{n!(n+2)!}.$$

The mean value of this distribution is calculated as,

$$\langle n\rangle=\frac{1}{N^{(\infty)}(J)}\sum_{n=0}^{\infty}\frac{2J^n}{(n-1)!(n+2)!}. \tag{35}$$

The unitary operator, $\hat{U}^{(\infty)}(t)$, defined as time evolution operator and given in (20) leads us to the time evolved GK CS for $k=\infty$. Hence, the operation of $\hat{U}^{(\infty)}(t)$ on the initial state given in (34), provides us time dependent GK CS as,

$$\left|(J,\theta)^{(\infty)},t\right\rangle = \frac{1}{\sqrt{N^{(\infty)}(J)}}\sum_{n=0}^{\infty}\frac{J^{\frac{n}{2}}e^{-in(n+2)(\theta+\omega^{(\infty)}t)}}{\sqrt{n!(n+2)!}}|n\rangle. \tag{36}$$

In contrast to $|(J,\theta)^{(2)},t\rangle$, the phase of the time evolved states, $|(J,\theta)^{(\infty)},t\rangle$, possesses a nonlinear dependence on quantum number n. The classical period for these states is

$$T_{cl}^{(\infty)}=\frac{1}{\pi(\langle n\rangle+1)}. \tag{37}$$

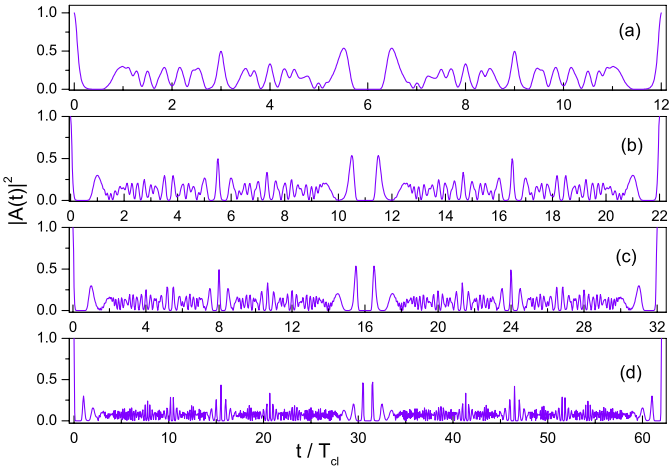

Fig. 3 We show modulus square of autocorrelation function, $|A(t)|^2$, given in (22) as a function of time, t, for infinite square well ($k \to \infty$) for: (**a**) $J = 38.05$, (**b**) $J = 125.6$, (**c**) $J = 263.1$, and (**d**) $J = 975.61$

The nonlinearity of the energy spectrum introduces a dephasing effect in adjacent terms of the summation which leads to the dispersion after a few classical periods, thus, GK CS observes collapse as the phase difference maximizes. Later, a restructuring of these states takes place as all contributing terms in the summation display a phase matching which results in the reconstruction of the initial state, at the time of revival, given as

$$T_{rev}^{(\infty)} = \frac{2}{\pi}. \tag{38}$$

The quantum mechanical revival time, $T_{rev}^{(k)}$, is inversely proportional to the difference of frequencies between adjacent n values. For $k = \infty$ the difference between frequencies become constant which as a consequence makes $T_{rev}^{(\infty)}$, independent of $\langle n \rangle$ and a constant, and $T_{sr}^{(\infty)} = \infty$. The phenomena of collapse and revival for GK CS of infinite square well is shown in Fig. 3.

As discussed earlier, the classical period and quantum revival time for GK CSs of power-law potentials depend on parameter J through the mean value, $\langle n \rangle$, of the weighting distribution, such that, $\langle n \rangle$ has direct proportion with J as given in (35) and shown in Fig. 1. Therefore, the classical period, $T_{cl}^{(\infty)}$, given in (37), displays an inverse proportionality on J. Equation (38), however, shows that quantum revival time, $T_{rev}^{(\infty)}$, is independent of $\langle n \rangle$ and, therefore, does not exhibit any dependence on J. This fact leads us to conclude that for the higher values of J, revival of GK CS occur after larger number of classical periods and vice versa, as seen in Fig. 3.

We present the probability distribution as function of space, at $t = 0$, for different values of J, as shown in Fig. 4. We note that increasing values of J shift the center of the initial state towards the left wall and lead to a narrower localization in space. Moreover, a single peak of initial probability density at lower values of J splits into multiple peaks as J increases. The spatio-temporal evolution of GK CS of the infinite square well displays the manifestation of constructive and destructive interferences which is governed by the time-dependent

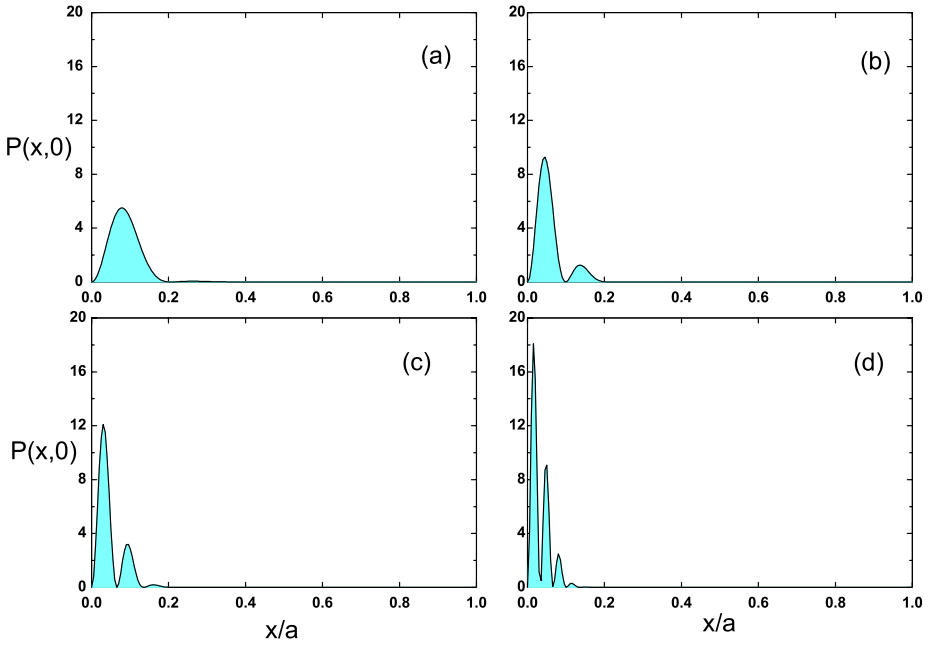

Fig. 4 Initial spatial localization of GK CS of infinite square well, $P(x,0) = |\langle x|(J,\theta)^{(\infty)}\rangle|^2$, for: (**a**) $J = 38.05$, (**b**) $J = 125.6$, (**c**) $J = 273.1$, and (**d**) $J = 975.61$

interference term, that is,

$$\mathrm{Re}\left[\frac{4}{aN^{(\infty)}(J)}\sum_{m\neq n}^{\infty}\frac{J^{\frac{(n+m)}{2}}}{\sqrt{\rho_n^{(\infty)}\rho_m^{(\infty)}}}\sin\left(\frac{n\pi x}{a}\right)\sin\left(\frac{m\pi x}{a}\right)e^{-i(e_n^{(\infty)}-e_m^{(\infty)})(\theta+\omega^{(\infty)}t)}\right],$$

as shown in Fig. 5. Hence, we observe that GK CS of the infinite square well potential display collapse and later in time develops fractional revivals and revivals.

4.3 Triangular Well Potential

Power-law potentials for $k = 1$, and $V_0/a = mg$, define a triangular well potential with an infinite wall at $x = 0$ where $x > 0$ as the accessible region. In this situation, we define the dimensionless eigenenergy $e_n^{(1)}$ from (9), such that, $e_n^{(1)} = (n + 3/4)^{2/3} - (3/4)^{2/3} \simeq (n)^{2/3}$, whereas the parameter $\rho_n^{(1)}$ is $\rho_n^{(1)} = (n!)^{2/3}$. The GK CS of triangular well potential take the form

$$\left|(J,\theta)^{(1)}\right\rangle = \frac{1}{\sqrt{N^{(1)}(J)}}\sum_{n=0}^{\infty}\frac{J^{\frac{n}{2}}e^{-in^{2/3}\theta}}{\sqrt{(n!)^{2/3}}}|n\rangle, \tag{39}$$

where the normalization constant is given as

$$N^{(1)}(J) = \sum_{n=0}^{\infty}\frac{J^n}{(n!)^{2/3}},$$

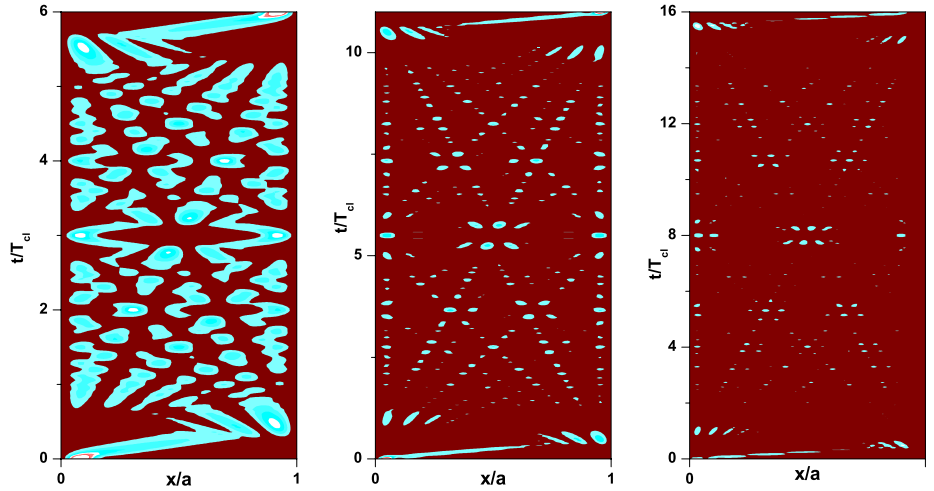

Fig. 5 Contour plots of the probability density $P(x,t)$ that show the space-time evolution of states, $|(J,\theta)^{(\infty)}\rangle$, for: (**a**) $J = 38.05$, (**b**) $J = 125.6$ and (**c**) $J = 263.1$

and the weighting distribution of these states is

$$|c_n^{(1)}|^2 = \frac{J^n}{N^{(1)}(J)(n!)^{2/3}}.$$

In addition, the mean value, $\langle n\rangle$, is

$$\langle n\rangle = \frac{1}{N^{(1)}(J)} \sum_{n=0}^{\infty} \frac{nJ^n}{(n!)^{2/3}}. \tag{40}$$

The unitary operator $\hat{U}^{(1)}(t)$ transforms the states in (39) into

$$\left|(J,\theta)^{(1)},t\right\rangle = \frac{1}{\sqrt{N^{(1)}(J)}} \sum_{n=0}^{\infty} \frac{J^{\frac{n}{2}} e^{-in^{(2/3)}(\theta+\omega^{(1)}t)}}{\sqrt{(n!)^{2/3}}} |n\rangle \tag{41}$$

which shows that the phase term has a nonlinear dependence on quantum number, n. Therefore, GK CS of triangular well potential observes collapse in the course of its time evolution, after few classical periods, as displayed in Fig. 6. The classical period $T_{cl}^{(1)}$, quantum revival time, $T_{rev}^{(1)}$, and super revival time, $T_{sr}^{(1)}$, for these states, respectively, are

$$T_{cl}^{(1)} = \frac{3\pi}{\omega^{(1)}} (\langle n\rangle)^{1/3}, \tag{42}$$

$$T_{rev}^{(1)} = \frac{18\pi}{\omega^{(1)}} (\langle n\rangle)^{4/3}, \tag{43}$$

$$T_{sr}^{(1)} = \frac{81\pi}{2\omega^{(1)}} (\langle n\rangle)^{7/3}. \tag{44}$$

In contrast to the harmonic oscillator and infinite square well, GK CS of triangular well potential has $T_{cl}^{(1)}$ and $T_{rev}^{(1)}$ which depend on mean value $\langle n\rangle$ of initial distribution and,

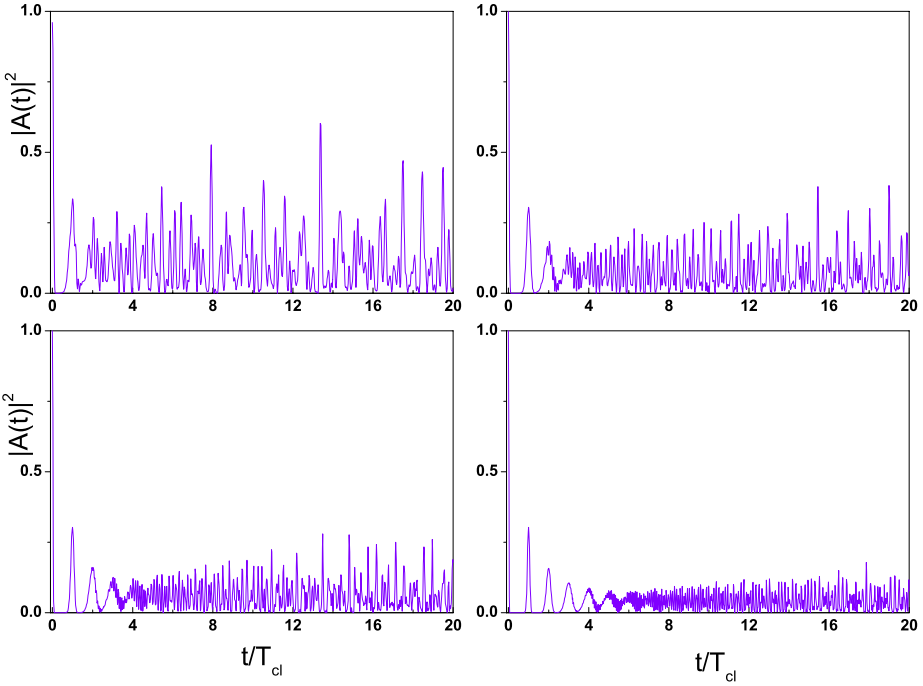

Fig. 6 We show modulus square of autocorrelation function, $|A(t)|^2$, given in (22) as a function of time, t, upto first twenty classical periods for ($k = 1$) and: (**a**) $J = 2.82$, (**b**) $J = 4.56$, (**c**) $J = 6.01$, and (**d**) $J = 9.61$

therefore, depend on parameter J, as given in (40). However, the dependence of $T_{rev}^{(1)}$ on $\langle n\rangle$ and, as a consequence on J, is higher than that of $T_{cl}^{(1)}$, since, $T_{cl}^{(1)} \propto (\langle n\rangle)^{1/3}$ and $T_{rev}^{(1)} \propto (\langle n\rangle)^{4/3}$. Hence, as the value of J increases the collapse and then revival of the initial GK CS occur after larger number of classical periods and vice versa, as displayed in Fig. 6. In the triangular well potential, however, we do not find exact revival of the initial state at time $t = T_{rev}^{(1)}$ which is due to the relative importance of higher order terms in the expansion in (26). Moreover, from (42) and (43), we find the interdependence of $T_{cl}^{(1)}$ and $T_{rev}^{(1)}$, that is, $T_{rev}^{(1)} = 6T_{cl}^{(1)}\langle n\rangle$.

In Fig. 7 we show the probability density of state $|(J,\theta)^{(1)}\rangle$, after different evolution times. It is seen that probability density at $t = 0$ exhibit a single peak that splits into multiple-peaks after few classical periods. The subsequent dynamics of these multiple-peaks interfere with each other and results in the collapse of the initial states. The interference is governed by the time-dependent part of the probability density,

$$2\,\mathrm{Re}\left[\frac{1}{N^{(1)}(J)}\sum_{m\neq n}^{\infty}\frac{J^{\frac{(n+m)}{2}}}{\sqrt{\rho_n^{(1)}\rho_m^{(1)}}}\psi_n(\zeta)\psi_m^*(\zeta)e^{-i(e_n^{(1)}-e_m^{(1)})(\theta+\omega^{(1)}t)}\right],$$

where, $\psi_n(\zeta) = N_n\,\mathrm{Ai}(\zeta - \zeta_n)$, and, $\zeta = x/x_0$, is the rescaled position. The resulting space-time dynamics is displayed in Fig. 8 by means of a quantum carpet which shows a gradually dominatory destructive interference, beyond $t = 0$, which results in the collapse of GK CS.

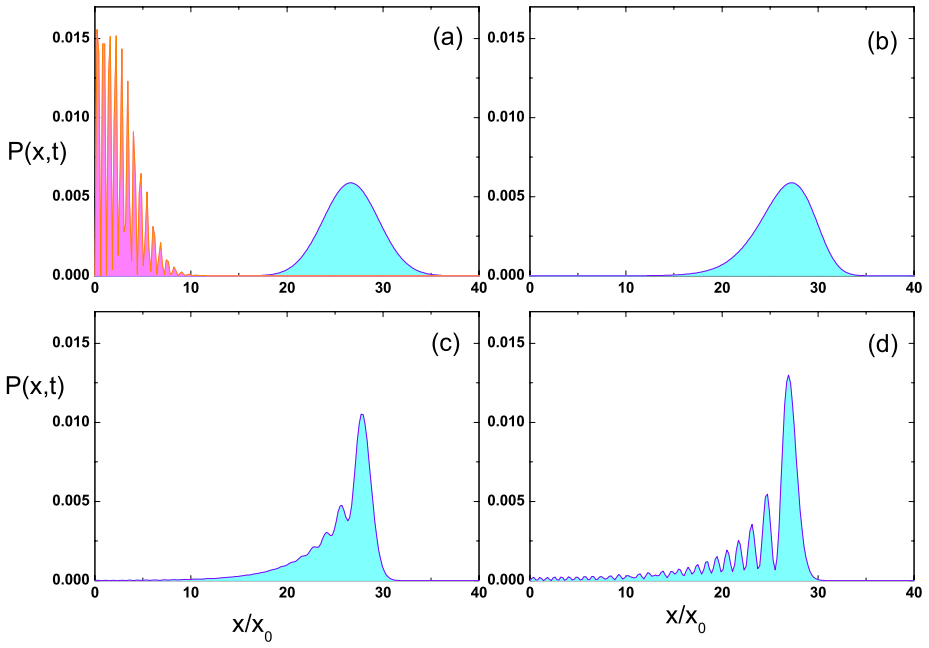

Fig. 7 (Color online) We show probability density function, $P^{(1)}(x,t) = |\langle x|e^{-i\omega^{(1)}\hat{X}_N^{(1)}t}|(J,\theta)^{(1)}\rangle|^2$ for triangular well potential after different evolution times: (**a**) $t = 0$ (*blue*) and $t = 1/2T_{(cl)}^{(1)}$ (*pink*), (**b**) $t = 1T_{(cl)}^{(1)}$ (**c**) $t = 2T_{(cl)}^{(1)}$, (**d**) $t = 3T_{(cl)}^{(1)}$

5 Discussion

We have constructed Gazeau-Klauder coherent states for a variety of Hamiltonian systems defined by power-law exponents: the harmonic oscillator, the infinite square well, and the triangular well potential, where the last two become the examples of, respectively, tightly binding potentials and loosely binding potentials of power-law potentials. The Gazeau-Klauder coherent states, $|(J,\theta)^{(k)}\rangle$, fulfill the requirements of normalization, continuity in both parameters J and θ, resolution of unity, and action identity. We study the dynamical characteristics of these states by using the auto-correlation function and the probability density function. We show that GK CSs follow nondispersive dynamics as long as underlying energy spectrum of the system is linear, that is, for GK CS of the harmonic oscillator, in general, however, they disperse after few classical periods and a gradual dephasing between contributing terms in the probability density leads to a collapse. Many classical periods latter, a revival of initial state takes place under the condition of phase matching. The effect of anharmonicity of the energy spectrum is shown by space-time evolution of the probability density which leads to the formation of space-time interference structures as quantum carpets [21, 22]. Hence, quantum states constructed following the Gazeau-Klauder formalism display dispersive behavior as a consequence of nonlinear dependence of energy on quantum number n of the corresponding system.

Acknowledgements We gratefully acknowledge valuable discussions with J.P. Gazeau, Y. Hassouni, E.M. Curado, M.A. Monteiro, M. Sadiq. SI thanks J.-M. Rost for hospitality at the Max-Planck Institute for the Physics of Complex Systems in Dresden, Germany and the Higher Education Commission, Pakistan for funding through grant 041203721E-026.

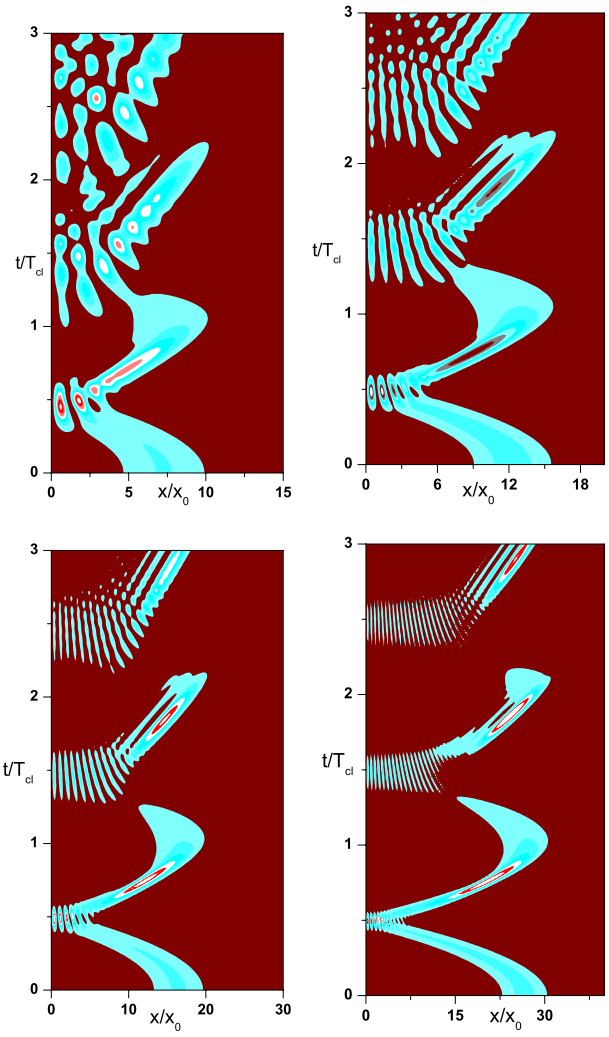

Fig. 8 We show contour plots of probability density of GK CS of triangular well potential for: (**a**) $J = 2.82$, (**b**) $J = 4.56$, (**c**) $J = 6.01$, and (**d**) $J = 9.61$. The *bright regions* in these carpets represent the maximum probabilities and *dark regions* represent the minimum probabilities

References

1. Schrödinger, E.: Naturwissenschaften **14**, 664 (1926)
2. Glauber, R.J.: Phys. Rev. Lett. **10**, 277 (1963)
3. Glauber, R.J.: Phys. Rev. **130**, 2529 (1963)
4. Glauber, R.J.: Phys. Rev. **131**, 2766 (1963)
5. Klauder, J.R., Skagerstam, B.S.: Coherent States: Applications in Physics and Mathematical Physics. Singapore, World Scientific (1985)
6. Perelomov, A.M.: Generalized Coherent States and Their Applications. Springer, Berlin (1986)
7. Glauber, R.J.: Quantum Theory of Optical Coherences. Wiley, New York (2007)
8. Gazeau, J.P.: Coherent States in Quantum Physics. Wiley, New York (2009)
9. Barut, A.O., Girardello, L.: Commun. Math. Phys. **21**, 41 (1971)
10. Perelomov, M.: Commun. Math. Phys. **26**, 222 (1972)
11. Klauder, J.R.: J. Math. Phys. **4**, 1055 (1963)
12. Klauder, J.R.: J. Phys. A: Math. Gen. **29**, L293 (1996)
13. Bellomo, P., Stroud, C.R.: J. Phys. A: Math. Gen. **31**, L445 (1998)
14. Gazeau, J.P.G., Klauder, J.R.: J. Phys. A: Math. Gen. **32**, 123 (1999)

15. Popov, D., Sajfert, V., Zaharie, I.: Physica A **387**, 4459 (2008)
16. Chenaghlou, A., Faizy, O.: J. Math. Phys. **49**, 022104 (2008)
17. Angelova, M., Hussin, V.: J. Phys. A: Math. Gen. **41**, 304016 (2008)
18. Antoine, J.P., Gazeau, J.P.G., Monceau, P., Klauder, J.R., Penson, K.A.: J. Math. Phys. **42**, 2349 (2001)
19. Hollingworth, J.M., Konstadopoulou, A., Chountasis, S., Vourdas, A., Backhouse, N.B.: J. Phys. A: Math. Gen. **34**, 9463 (2001)
20. Iqbal, S., Qurat-ul-Ann, Saif, F.: Phys. Lett. A **356**, 231 (2006)
21. Großmann, F., Rost, J.-M., Schleich, W.P.: J. Phys. A: Math. Gen. **30**, L227 (1997)
22. Marzoli, L., Saif, F., Bialynicki-Birula, I., Friesch, M.O., Kaplan, A.E., Schleich, W.P.: Acta Phys. Slovaca **48**, 323 (1998)
23. Sukhatme, U.P.: Am. J. Phys. **41**, 1015 (1973)
24. Wallis, H., Dalibard, J., Cohen-Tannoudji, C.: Appl. Phys. B **54**, 407 (1991)
25. Gea-Banacloche, J.: Am. J. Phys. **67**, 776 (1999)
26. Klauder, J.R., Penson, K.A., Sixdeniers, J.-M.: Phys. Rev. A **64**, 013817 (2001)
27. Nauenberg, M.: J. Phys. B: At. Mol. Opt. Phys. **23**, L385 (1990)
28. Robinett, R.W.: Phys. Rep. **392**, 1 (2004)
29. Buchleitner, A., Delande, D., Zakrzewskix, J.: Phys. Rep. **368**, 409 (1990)